Disease Markers 24 (2008) 41–50
IOS Press

GPR87 is an overexpressed G-protein coupled receptor in squamous cell carcinoma of the lung

Mathias Gugger[a], Richard White[b], Susan Song[b], Bea Waser[a], Renzo Cescato[a], Pierre Rivière[b] and Jean Claude Reubi[a,*]
[a]*Division of Cell Biology and Experimental Cancer Research, Institute of Pathology, University of Bern, Murtenstrasse 31, 3010 Bern, Switzerland*
[b]*Ferring Research Institute, 3550 General Atomics Court, Building 2, Room 442, San Diego, CA 92121, USA*

Abstract. Lung cancer is the leading cause of cancer death worldwide. The overall 5-year survival after therapy is about 16% and there is a clear need for better treatment options, such as therapies targeting specific molecular structures. G-protein coupled receptors (GPCRs), as the largest family of cell surface receptors, represent an important group of potential targets for diagnostics and therapy. We therefore used laser capture microdissection and GPCR-focused Affymetrix microarrays to examine the expression of 929 GPCR transcripts in tissue samples of 10 patients with squamous cell carcinoma and 7 with adenocarcinoma in order to identify novel targets in non-small cell lung carcinoma (NSCLC). The relative gene expression levels were calculated in tumour samples compared to samples of the neighbouring alveolar tissue in every patient. Based on this unique study design, we identified 5 significantly overexpressed GPCRs in squamous cell carcinoma, in the following decreasing order of expression: GPR87 > CMKOR1 > FZD10 > LGR4 > P2RY11. All are non-olfactory and GRAFS (glutamate, rhodopsin, adhesion, frizzled/taste2, secretin family) classified. GPR87, LGR4 and CMKOR1 are orphan receptors. GPR87 stands out as a candidate for further target validation due to its marked overexpression and correlation on a mutation-based level to squamous cell carcinoma.

Keywords: Lung cancer, squamous cell carcinoma, molecular targets, tumour to background ratio, G-protein coupled receptor, cDNA microarray, laser capture microdissection, GPR87

1. Introduction

Lung cancer is the leading cause of cancer death worldwide [23] and is classified as either non-small cell lung carcinoma (NSCLC) or small cell lung carcinoma (SCLC). About 25% of lung carcinomas are SCLCs, representing one morphological type of a neuroendocrine carcinoma, are generally metastasized at the time of diagnosis and sensitive to classical chemotherapy. The remainder are NSCLCs, consisting primarily of adenocarcinoma or squamous cell carcinoma, which are amenable to surgery and adjuvant chemotherapy depending on the stage of the disease. Despite advances in imaging, diagnosis, staging, and treatment, the 5-year survival over all stages and after therapy remains around 16% and so the need for better diagnosis and treatment is obvious [32].

Overexpressed receptors at the tumour cell surface may represent specific targets for tumour diagnosis and treatment. For example, they can be targeted with specific radioactive or cytotoxic molecules for diagnosis or radiotherapy taking advantage of the ligand receptor complex internalization. G-protein coupled receptors (GPCR) constitute the largest receptor family with

*Corresponding author: Jean Claude Reubi, MD, Division of Cell Biology and Experimental Cancer Research, Institute of Pathology, University of Bern, PO Box 62, Murtenstrasse 31, CH-3010 Bern, Switzerland. Tel.: +41 31 632 3242; Fax: +41 31 632 8999; E-mail: reubi@pathology.unibe.ch.

ISSN 0278-0240/08/$17.00

more than 800 members known since the sequencing of the human genome project [5]. They are widely expressed in human tissues in an organ-specific manner [6] and they play a fundamental role in physiology and pathophysiology. Many of the currently marketed drugs are modulators of known GPCRs. Therefore, GPCRs overall are a primary focus of target validation [37].

In vitro, individual peptide receptors, belonging to the GPCR family, are often extremely abundant in specific cancers [27], but are rarely overexpressed in NSCLC, except for VPAC1 [29] or sst_2 in peritumoural veins [3]. In the clinic, sst_2 is the only peptide receptor that has been used as a target to visualize NSCLC, using the synthetic somatostatin analogues Octreoscan [11] and ^{111}In-DOTA-lanreotide [16,33]. But as opposed to gastro-entero-pancreatic tumours [13], this approach is not more reliable than conventional radiological techniques [1] possibly because of the low sst_2 expression. Furthermore, there is no established *in vivo* GPCR-based targeted therapy in NSCLC. In contrast, tyrosine kinase receptors are currently being targeted successfully by small molecule inhibitors in a small fraction of NSCLCs with amplification or gain-of-function mutations of the epidermal growth factor receptor gene [21].

To evaluate the possibilities of clinical applications for the genome-known GPCRs in NSCLC we have screened for overexpression of GPCRs in squamous cell carcinoma and adenocarcinoma, the most important histological types of NSCLC, using a microdissection-based cDNA microarray approach. We selected the surrounding alveolar tissue in every tumour as the RNA reference to get information about the tumour to background ratio in every patient. Laser capture microdissection allowed us to investigate specifically cancer cells which represent the primary clinical target. Based on this technique, peritumoural vessels as well as solid peri- or intratumoural inflammatory infiltrates could be excluded.

2. Material and methods

2.1. Tissue bank

We chose -80°C frozen and Tissue Tek® OCT medium (Sakura, Tokyo, Japan) embedded tissue samples of carcinoma and of normal lung tissue from patients with squamous cell carcinoma ($n = 10$) and adenocarcinoma ($n = 7$) out of a tissue bank from clinical lobectomy specimens frozen within maximally 30 min after removal from the patient. The patients did not have any neo-adjuvant chemotherapy prior to surgery. The diagnosis based on formalin-fixed and paraffin-embedded tissue blocks from the same specimen. Table 1 summarizes the patient characteristics. The tissue use was approved by the local ethic committee. 16 μm thick frozen sections on glass slides followed by 7 μm thick sections were prepared on a cryostat (Leitz) from each frozen tissue block. A 7 μm thick section was HE-stained to provide an overview of the tissue morphology prior to the microdissection procedure.

2.2. Laser capture microdissection

The 16 μm thick frozen sections for microdissection were handled in disposable, polypropylene cytology mailers for 4 slides and fixed in 75% EtOH for 45 s; Tissue Tek® OCT medium was removed in water two times for 30 s and the tissue was dehydrated in 75% EtOH for 45 s, 95% EtOH for 45 s, 100% EtOH for 1 min and in Xylene shortly to remove larger amounts of EtOH and then for 3 min. The water used in all steps was RNAse free. The section was then air dried for 5 min. We used the PixCell II LCM System from Arcturus Engineering (Mountain View, CA, USA). The microdissection was performed by manually initiating the laser pulses under optical control (Fig. 1b) by the main investigator (M.G.). The laser spot size was 30 μm with 6 ms pulse duration at a power of 40 mW. Only intact tumour tissue was dissected and necrotic areas as well as peri- and intratumoural stromal compartments were left out (Fig. 1a).

2.3. RNA extraction, RNA amplification, cDNA microarray procedure

RNA was extracted with the Qiagen RNA Microkit® (Valencia, CA, USA) and eluted in 14 μl RNAse free water. The quality and the amount of total RNA was measured by the Agilent BioAnalyzer2100 (Palo Alto, CA, USA) for each sample (Fig. 1c). We performed reverse transcription and T7 amplification with the MessageAmp^{TM} Kit from Ambion® (Woodward, TX, USA) to get a two round aRNA. We chose 50 ng of total RNA as the input. Biotinylization and fragmentation of the aRNA for target preparation, addition of hybridization controls and hybridization to the microarray probe cells was performed according to the Affymetrix® Eukaryotic Sample and Array Processing Manual (Santa Clara, CA, USA).

Table 1
Characteristics of patient's lung carcinomas

ID	Diagnosis	grade	gender	age	TNM-stage
285	Squamous Cell Carcinoma	G2/3	f	71	pT2 pN1 cM0
288	Squamous Cell Carcinoma	G2/3	m	53	pT2 pN1 cM0
290	Squamous Cell Carcinoma	G3	m	72	pT3 pN1 cM0
291	Squamous Cell Carcinoma	G2/3	m	72	pT2 pN0 cM0
296	Squamous Cell Carcinoma	G2	m	72	pT2 pN0 cM0
300	Squamous Cell Carcinoma	G2	m	75	pT3 pN2 cM0
302	Squamous Cell Carcinoma	G3	m	73	pT1 pN0 cM0
306	Squamous Cell Carcinoma	G2	m	73	pT2 pN1 cM0
309	Squamous Cell Carcinoma	G2	m	63	pT2 pN1 cM0
315	Squamous Cell Carcinoma	G3	m	66	pT2 pN0 cM0
262	Adenocarcinoma	G3	f	50	pT4 pN1 cM0
265	Adenocarcinoma	G2	f	73	pT2 pN1 cM0
267	Adenocarcinoma	G2	f	52	pT2 pN0 cM0
269	Adenocarcinoma	G2	m	45	pT2 pN0 cM0
279	Adenocarcinoma	G2	m	56	pT1 pN0 cM0
280	Adenocarcinoma	G2	f	64	pT1 pN1 cM0
305	Adenocarcinoma	G3	m	57	pT3 pN1 cM0

Abbreviations: ID = sample identification; f = female; m = male.

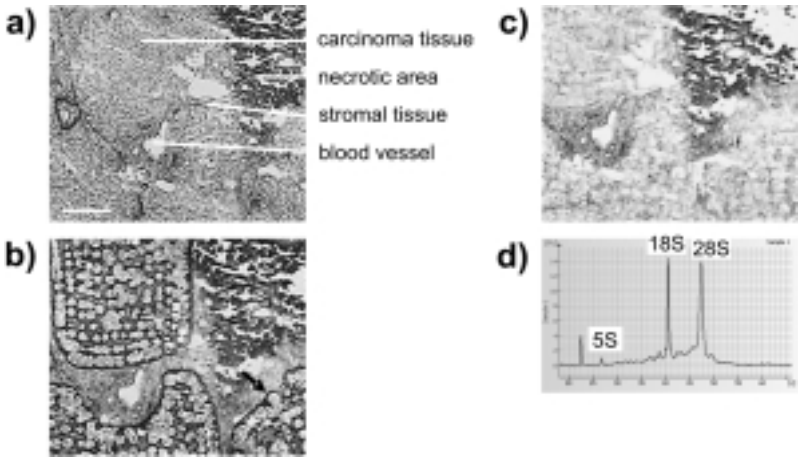

Fig. 1. Unstained 16 μm thick tissue slide (a, bar = 100 μm) depicting carcinoma tissue, a necrotic area, a blood vessel and stromal tissue. The laser beam was directed and pulsed under optical control through a cap. Each laser pulse lowered a spot (arrow) of an energy-sensitive film at the lower side of the cap onto the tissue (b). After removal of the cap the remaining tissue on the glass slide is visible (c). The electropherogram (d) depicts a good quality of the extracted total mRNA with a ratio 28S:18SrRNA = 1.8 and a low baseline between 18S and 5S.

2.4. Acquisition and analysis of cDNA microarray data

We used a custom-designed (Ferring Research Institute, San Diego, USA) in situ cDNA Affymetrix® microarray with 929 GPCR probe cells. Signal intensities were detected on an Agilent GeneArray® Scanner and the raw data was acquired and standardized with Affymetrix® Microarray Suite Software Version 5.0. We considered only genes with expression levels qualified as present or marginal in the Affymetrix report in more or equal than 50% of normal or carcinoma samples. The microarray data was then analyzed using GeneSifter® Software (vizXlabs, Seattle, WA, USA) by class comparison with a standard t test on the $\log_2$ of the all mean normalized intensity values. We arbitrarily chose a 3-fold threshold for overexpression in the cancer cells. The p-values were corrected for false-discovery rates to < 0.05 by the Benjamini and Hochberg algorithm.

2.5. Quality control measures for the microarray procedure and the data analysis

We can emphasize the following quality control issues: The main investigator (M.G.) maintained the tis-

sue bank, he controlled the HE sections and he did all the microdissection work. RNA quantity and quality was measured by the Agilent BioAnalyzer2100 for a few samples before and for all samples for every main step after microdissection. The 28S:18S ratios of the total RNA for all samples were > 1.0 and the baseline between the 18S and 5S rRNA was low, being within the recommended limits for a suitable RNA quality [22]. The Affymetrix® microarrays were all out of the same production batch. The correction for false-discovery rates allowed an appropriate conclusion about the significance of the differential expression of a transcript to be made. In comparison to tissue based studies laser capture microdissection studies generate small total RNA amounts and necessitate RNA amplification to get enough amounts of cDNA for the hybridization of the microarrays. This amplification step is not a source of errors, because the sensitivity of differential transcription profiles can even be enhanced compared to non-amplified RNA [25].

2.6. Confirmatory quantitative RT-PCR

Because we did use up the total RNA of some samples completely for the cDNA microarray procedure, we microdissected all samples again out of the same tissue blocks for confirmatory quantitative RT-PCR (SYBR Green method, MJ Research Opticon 2 machine, Genetic Technologies, Miami, FL, USA). The extracted total RNA was one round amplified as described above to have a large enough quantity for future investigations. We focused on the most siginificant cDNA microarray result and did the quantative RT-PCR for GPR87 (Primers: Based on NCBI Accession Nb: NM_023915/F: (74–99) 5'-cta cct tgt ctg gta ggg gag atg t-3'/R: (292–267) 5'-tca gca tag gtt att cct ggt ttg a-3'/Annealing Temperature 63 °C/PCR length 168 base pairs spanning the only two exons). To analyze the quantitative RT-PCR data we applied the $\Delta\Delta$Ct method.

2.7. Western blotting and immunohistochemistry

Western blotting with the only two available commercial antibodies NLS 1580 (N-terminal, Novus Biologicals, Littleton, CO, USA) and NLS 1584 (C-terminal, Novus Biologicals) against GRP87 was performed on frozen tumor tissue samples (approx. 50 mg) as previously described [28]. We investigated the three squamous cell carcinoma samples with the highest overexpression fold. We included prostate, thymus and placental tissues as tissues that may express GPR87 [14, 38]. The proteins from the described sources were analysed by SDS-PAGE. For both antibodies the peptide immunogens were available for preimmune absorption steps to distinguish specific bands. Additionally, we performed deglycosylation steps to check the change of location of potential specific bands in the gel.

Immunohistochemistry was performed on frozen and formalin-fixed, paraffin-embedded tissue of the above stated three squamous cell carcinoma samples as described previously [28]. Several different pretreatments, like trypsin or pronase digestion, microwave oven or pressure cooking boiling in citrate buffer were performed for antigen retrevial. For both antibodies the peptide immunogens were available for preimmune absorption steps to distinguish specific staining.

3. Results

Laser capture microdissection was applied, as described in Material and Methods, on all samples successfully (Fig. 1). During one hour the tissue on the glass slides remained dry enough, allowing the microdissection of an area of up to 3 MacroCaps®. The estimated fraction of tissue adhering to the cap was between 80% and 50% (Fig. 1b and 1c). The amount of total RNA was between 4–37 ng/μl for the alveolar tissue samples and 15–177 ng/μl for the lung cancer tissue samples. The quality of the extracted total mRNA was within the recommended limits (Fig. 1d).

The analysis of the cDNA microarray data shows that among the 929 GPCR transcripts tested, five of them are overexpressed significantly ($p < 0.05$, Benjamini and Hochberg's false-discovery rate correction applied) in squamous cell carcinoma or adenocarcinoma in comparison to the individual alveolar tissue samples (Table 2 and Fig. 2). These are GPR87, CMKOR1, FZD10, LGR4 and P2RY11. GPR87, LGR4 and CMKOR1 are orphan receptors. All are non-olfactory and GRAFS-classified. The GRAFS-classification [5] is based on phylogenetic relationships of non-olfactory GPCRs and contains 5 families, named glutamate, rhodopsin, adhesion, frizzled/taste2, and secretin with 319 GPCRs. GPR87 and P2RY11 are purin receptors, LGR4 is a glycoprotein receptor and CMKOR1 is a chemokine receptor, all belonging to the rhodopsin family; FZD10 is a frizzled receptor, belonging to the frizzled/taste2 family.

The standard t test without p-value restriction identifies 113 differentially expressed GRAFS genes in the

Table 2
$>$ 3-fold overexpressed G-protein coupled receptors compared to alveolar tissue

Gene Identifier	Accession Nb	Squamous cell carcinoma $n = 10$ fold overexpression*	corrected p-value**	Adenocarcinoma $n = 7$ fold overexpression*	corrected p-value**
GPR87	NM_023915	17.06	0.0002	–	
CMKOR1	XM_051522	4.56	0.00049	–	
FZD10	NM_007197	3.66	0.032	–	
LGR4	NM_018490	3.19	0.0011	3.78	0.045
P2RY11	NM_002566	3.11	0.0008	–	

*Standard t test on the $\log_2$ of the all mean normalized intensity values.
**Benjamini and Hochberg corrected p-values < 0.05.

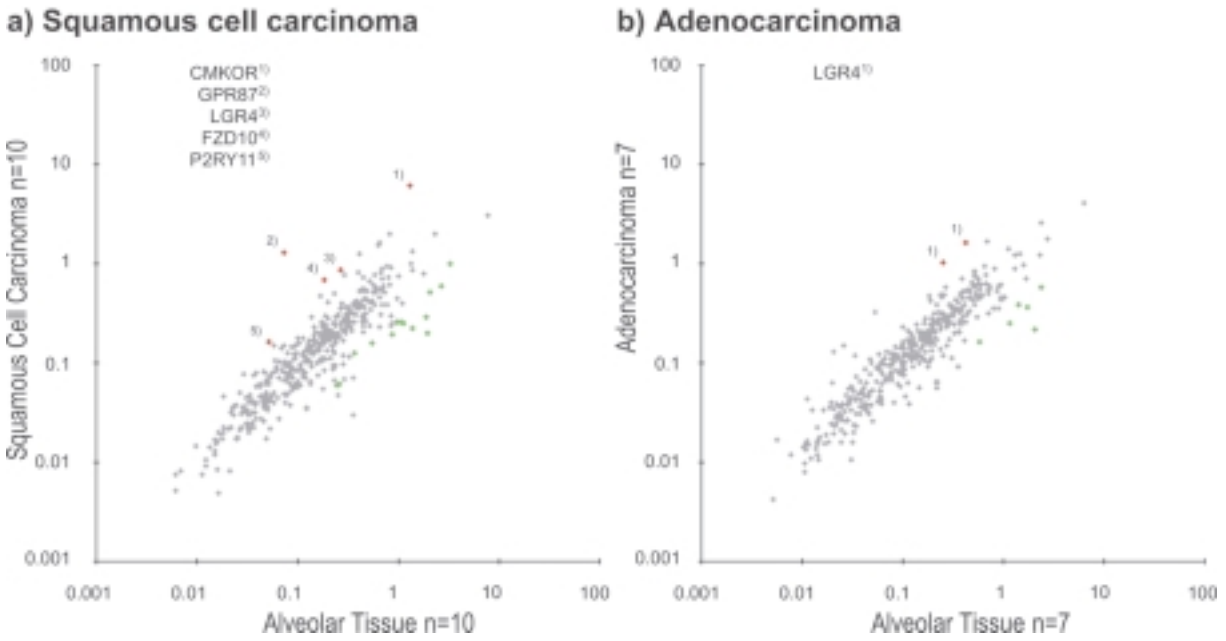

Fig. 2. Scatter plot analysis comparing expression hybridization from microdissected squamous cell carcinomas (a) or adenocarcinomas (b) (y-axis) with the microdissected corresponding alveolar tissues (x-axis). Differentially expressed GRAFS-receptor genes are depicted based on the standard t test on $\log_2$ of the all mean normalized intensity values of the hybridized probe cells. Significantly upregulated (and by $>$ 3-fold) (✚) or down-regulated (and by $>$ 3-fold) (✚) receptor transcripts are labelled after strengthening of the data set by correction of the p-values with the Benjamini and Hochberg algorithm for false-discovery rates to < 0.05. This is an overall representation of data; fractions of these data are detailed in Tables 2 and 3.

squamous carcinoma samples and 100 in the adenocarcinoma samples respectively. These genes are depicted in the scatter plots for squamous cell carcinoma and adenocarcinoma respectively (Fig. 2). With p-value restriction to < 0.05 60 of them are still qualified as significantly differentially expressed in squamous cell carcinoma samples and 26 in adenocarinoma samples. The majority of them, 46 receptors in squamous cell carcinoma and 22 in adenocarcinoma, are down regulated. With further p-value restriction for false-discovery rates with the Benjamini and Hochberg algorithm to < 0.05 52 of them are still qualified as significantly differentially expressed in squamous cell carcinoma and 9 in adenocarcinoma (Table 3). With the application of the same criteria we did not find significantly overexpressed olfactory GPCRs (data not shown).

The signature of these five significantly overexpressed receptors differs for squamous cell carcinoma compared to adenocarcinoma (Table 2 and Fig. 2). In the former, all five are represented, whereas in the latter only LGR4 is present.

Quantitative RT-PCR on the newly microdissected samples out of the same tissue blocks used for cDNA microarrays confirms the cDNA microarray data for GPR87 (Fig. 3). 18S rRNA gene expression was equal

Table 3
Differentially expressed GRAFS-classified G-protein coupled receptors compared to alveolar tissue

		Squamous cell carcinoma $n = 10$		Adenocarcinoma $n = 7$	
		fold differential expression*		fold differential expression*	
Gene Identifier	Accession Nb		corrected p-value**		corrected p-value**
Secretin Receptor Family					
CALCRL	NM_005795	−2	0.034	–	
SCTR	NM_002980	−2.92	0.0000091	–	
VPAC1	NM_004624	−2.81	0.0008	−3.75	0.011
Adhesion Receptor Family					
BAI3	NM_001704	−2.57	0.011	–	
CD97	NM_078481	−6.74	0.00000023	−2.44	0.045
EMR1	NM_001974	−1.83	0.01	–	
ETL	NM_022159	−4.6	0.00016	–	
GPR56	NM_005682	2.37	0.0013	–	
Glutamate Receptor Family					
GABBR1	NM_021903	−1.43	0.00084	–	
Frizzled/Taste Receptor Family					
FZD4	NM_012193	−3.35	0.0000011	–	
FZD6	NM_003506	2.43	0.0069	–	
FZD7	NM_003507	2.38	0.032	–	
FZD10	NM_007197	3.66	0.032	–	
Rhodopsin Family α-Group					
Prostaglandin Receptor Cluster					
PTGER2	NM_000956	−12.2	0.000025	–	
PTGFR	NM_000959	−3.02	0.00052	–	
Amin Receptor Cluster					
ADRB2	NM_000024	−4.19	0.0000042	−4.27	0.0072
CHRM3	NM_000740	1.97	0.0083	–	
Opsins Receptor Cluster					
OPN1MW	NM_000513	2	0.045	–	
MECA Receptor Cluster					
ADORA3	NM_000677	−1.47	0.013	–	
ADORA2B	NM_000676	2.09	0.011	–	
EDG8	NM_030760	2.59	0.00042	–	
EDG5	NM_004230	−1.61	0.035	–	
EDG1	NM_001400	−3.85	0.000049	−2.32	0.011
Rhodopsin Family β-group					
EDNRB	NM_000115	−10	0.00019	−9.72	0.0017
EDNRA	NM_001957	−4.6	0.00011	–	
NPY1R	NM_000909	−2.13	0.022	–	
Rhodopsin Family γ-group					
SSTR3	NM_001051	1.32	0.0069	–	
SSTR1	NM_001049	−5.35	0.0019	–	
Chemokine Receptor Cluster					
CMKOR1	XM_051522	4.56	0.00049	–	
AGTR1	NM_031850	−6.25	0.0000000019	−4.69	0.00091
CXCR4	NM_003467	−2.6	0.025	–	
CCRL2	NM_003965	−3.56	0.00013	−3.58	0.0017
CXC3R1	NM_001337	−4.52	0.00000064	−4.82	0.0017
CCR1	NM_001295	−1.66	0.038	–	
CCR2	NM_000647	−1.91	0.028		
CXCR2(IL8RB)	NM_001557	−2.12	0.00049	–	
C5R1	NM_001736	−4.29	0.0011	–	
FPR1	NM_002029	−2.23	0.0013	–	
FPRL1	NM_001462	−4.39	0.002	–	
Rhodopsin Family δ-group					
Glycoprotein Receptor Cluster					
LGR7	NM_021634	−2.41	0.011	–	
LGR4	NM_018490	3.19	0.0011	3.78	0.045

Table 3, continued

Gene Identifier	Accession Nb	Squamous cell carcinoma $n = 10$ fold differential expression*	corrected p-value**	Adenocarcinoma $n = 7$ fold differential expression*	corrected p-value**
Purin Receptor Cluster					
PTAFR	NM_000952	−1.56	0.0066	–	
EBI2	NM_004951	−3.52	0.002	–	
P2RY11	NM_002566	3.11	0.0008	–	
C3AR(C3AR1)	NM_004054	−2.91	0.004	–	
GPR87	NM_023915	17.1	0.0002	–	
GPR105	NM_014879	−4.22	0.000025	–	
FKSG(GPR86,GPR94)	NM_023914	−2.24	0.0008	–	
CYSLT1	NM_006639	−2.2	0.002	–	
P2RY1	NM_002563	2.73	0.013	–	
GPR65	NM_003608	−5.15	0.013	–	
H963(GPR171)	NM_013308	−2.32	0.024	–	

*Standard t test on the $\log_2$ of the all mean normalized signal intensity values.
**Benjamini and Hochberg corrected p-values < 0.05.
$>$ 3-fold overexpressed receptors in underlined letters.

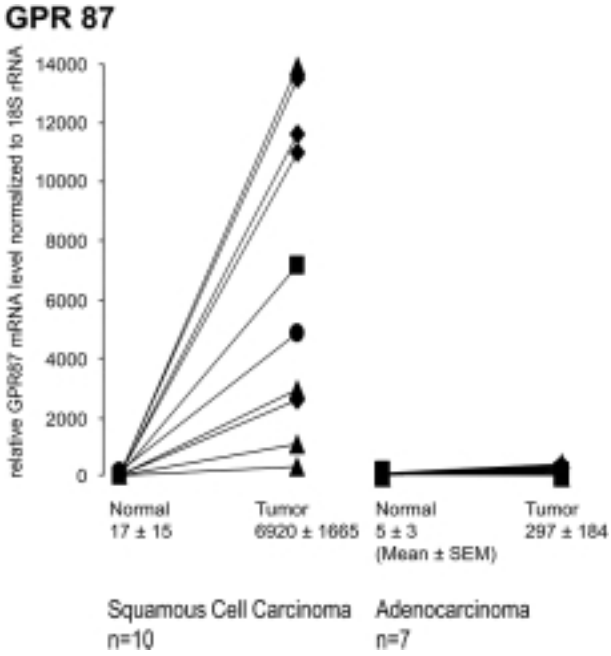

Fig. 3. Relative expression levels of GPR87 normalized to 18S rRNA gene in the carcinoma samples compared to the corresponding alveolar tissue. These data were generated on newly microdissected samples of the same tissues used for cDNA microarrays. GPR87 shows significantly higher relative expression levels in samples of squamous cell carcinoma compared to samples of adenocarcinoma. All alveolar tissue samples show a low relative expression level.

at a low level in carcinoma tissue and alveolar tissue and was used to normalize the data. Two issues are noteworthy. First, GPR87 shows higher relative expression levels in samples of squamous cell carcinoma compared to samples of adenocarcinoma. Second, all alveolar tissue samples show a low relative expression level.

In order to confirm the cDNA microarray and quantative RT-PCR results at the protein level we performed Western blottings for GPR87 with the two available commercial antibodies. However, despite a thorough testing including also external controls, no specific band corresponding to the GPR87 molecular characteristics could be found in the lung carcinoma samples, neither with NLS1580 nor with NLS1584. Immunohistochemistry with these two antibodies did not show any specific staining neither.

4. Discussion

By using laser capture microdissection under the guidance of a clinical pathologist, our cDNA microarray study was able to detect significantly overexpressed GPCRs in NSCLC. These are GPR87 [38], CMKOR1 [31], LGR4 [8], FZD10 [12] and P2RY11 [19], all overexpressed in squamous cell carcinoma or adenocarcinoma (Table 2, Fig. 2) of the lung. The majority of these receptors are not well known and their role in physiology and pathophysiology is poorly investigated. However, it is known that CMKOR1 is a coreceptor during HIV-Infection [31], that LGR4 plays an essential role for mouse embryonic growth as well as kidney and liver development [17], and that FZD10 is expressed specifically during mouse lung development [35]. P2RY11 as a nucleotide receptor is involved in many biological processes [4], among them the regulation of cell growth [30]. After the interrogation of the data [18] by the Benjamini and Hochberg algorithm for false-discovery rates in the strengthened data set, GPR87 stands out among the overexpressed GPCRs based on the highest statistical significance ($p = 0.0002$) and based on the highest fold-overexpression (17.1) (Table 2). However, for GPR87 there is no physiologic role known so far.

It has to be noted that our cDNA microarray study also identifies some significantly downregulated GPCRs (Table 3), for example PTGER2 in squamous cell carcinoma. Although not in the focus of our study, downregulated receptors may be as important for carcinogenesis as upregulated receptors. Indeed, PTGER2 has been reported to mediate growth stimuli in human lung adenocarcinoma [7]; its downregulation in squamous cell carcinoma therefore may point to differences in the carcinogenesis in these tumour types.

A unique study design based on the following three characteristics has been essential to obtain the present results. First, the use of laser capture microdissection; this technique allows dissection of the tissue on a cellular level and to collect a pure sample of carcinoma cells (Fig. 1), which represent the primary target of potential diagnostic or therapeutic applications. Other tumour compartments, like tumour-associated stroma, tumour-associated inflammatory infiltrates, peritumoural vessels or necrotic areas can be left out reliably with this technique (Fig. 1) compared to the use of whole tissue slides. The exclusion of peri- or intra-tumoural compartments is indeed not possible in whole tissue slides. This is important, because such tissue compartments play different pathophysiological roles in the tumour and represent therefore different targets. Second, the choice of the alveolar tissue as the RNA reference; this allows the evaluation of the clinically important tumour to background ratio [27]. The alveolar tissue constituting 81% of the total lung volume [36] is by far the largest volume fraction of the lung and represents the tumour background. The receptor density in the tumour and, as consequence, the tumour to background ratio, are important when a tumour is to be targeted with a radioligand binding to a receptor; the receptor of this ligand must be expressed in a sufficiently high density in the tumour but in an as low as possible density in the surrounding tissue, so that the radioligand produces its required effect in the tumour preferably. Third, the evaluation of the tumour tissue and the reference tissue in the same patient; this allows detection of the true differential gene expressions in every patient. Because tobacco smoke evokes gene aberrations not only in the tumour but anywhere in the lung tissue (field cancerization) [26], it is mandatory that the RNA reference is the individual alveolar tissue. A single RNA reference for all tumour samples [18], which is appropriate in studies investigating the gene expression signatures of different tumour types of the lung, would not detect a differential gene expression adequately in a smoker compared to a non-smoker.

Is there a known pathogenetic relationship between these overexpressed GPCRs and NSCLC? It is GPR87 that may give the most interesting answer to this question. Namely, at the level of genomic aberrations, GPR87 shows a striking association with squamous cell carcinoma of the lung. Indeed, the gene location 3q24 [38] lies in the region 3q24-qter with significant more gains and amplifications in squamous cell carcinoma compared to adenocarcinoma [24]. These genomic aberrations may well form the basis of the more abundant GPR87 expression in squamous cell carcinoma compared to adenocarcinoma. At the level of the potential role of these overexpressed receptors, it is of particular interest to note that GPR87 overexpression has been shown in testicular cancer as a probable downstream effect of chemotherapy-induced p53 [9]. This is so far the only evidence for a role of GPR87 in a particular cancer. The present study gives additional information regarding GPR87 overexpression; in squamous cell carcinoma of the lung, GPR87 overexpression is associated to gains of the corresponding genomic region [38]. These circumstances may point to a potential carcinogenetic role of GPR87 and are well worth further investigation. Conversely, there is no answer to the above-mentioned question for the other GPCRs

found overexpressed. In their gene locations [5,8,12, 15] no genomic gains in adenocarcinoma or squamous cell carcinoma are described [2,10,24]. FZD10 and P2RY11 are members of well known molecular pathways that are also associated to the pathogenesis of NSCLC [30,34], but their specific role in NSCLC is not known. Finally, for LGR4 and CMKOR1 no role in human cancer has been described so far.

Can we detect the GPR87 protein? GPR87 is a very recently discovered orphan receptor. Evaluation of the protein is difficult, not only because there are no natural ligands available to perform binding studies, but also because there are only a limited number of commercial antibodies available. There are not even established positive controls for immunohistochemical studies. We nevertheless have extensively evaluated the only two commercially available antibodies in the lung cancer samples, without success however. Western blots and immunohistochemistry, including all required control experiments as reported previously [28], were negative in all samples. This may not be so surprising given how difficult it is to generate antibodies that adequately identify GPCRs in human tissues. Searching for ligands or developing new antibodies for GPR87 will clearly be challenging projects for the near future. The recent discovery of endogenous surrogate ligands for human P2RY12 [20] to which GPR87 is phylogenetically tightly correlated may facilitate ligand-based investigative methods to find a natural ligand.

GPR87 appears to be the most promising candidate for further target validation among the overexpressed receptors in the present study. First, GPR87 is the only example of the overexpressed GPCRs that can be correlated on a mutation-based level to squamous cell carcinoma of the lung. This finding should trigger a more detailed investigation of a carcinogenetic role which may match GPR87 definitively with lung cancer, making it a validated target. Second, GPR87 shows by far the highest fold level of the overexpressed GPCRs. Because of the low GPR87 level in the alveolar tissue (Fig. 3) this can be translated into a high tumour to background ratio that represents an important prerequisite for a targeted therapy.

In conclusion, we have detected, in a cDNA microarray study focused on tumours of individual patients, five transcriptionally overexpressed GPCRs in NSCLC. One of these, GPR87 may be carcinogenetically associated to squamous cell carcinoma and should be further validated as a target of potential diagnostic, therapeutic or prognostic significance.

References

[1] J. Blum, H. Handmaker, J. Lister-James and N. Rinne, A multicenter trial with a somatostatin analog (99m)Tc depreotide in the evaluation of solitary pulmonary nodules, *Chest* **117** (2000), 1232–1238.

[2] M. Chujo, T. Noguchi, T. Miura, M. Arinaga, Y. Uchida and Y. Tagawa, Comparative genomic hybridization analysis detected frequent overrepresentation of chromosome 3q in squamous cell carcinoma of the lung, *Lung Cancer* **38** (2002), 23–29.

[3] B. Denzler and J.C. Reubi, Expression of somatostatin receptors in peritumoral veins of human tumors, *Cancer* **85** (1999), 188–198.

[4] G.R. Dubyak and C. el-Moatassim, Signal transduction via P2-purinergic receptors for extracellular ATP and other nucleotides, *Am J Physiol* **265** (1993), C577–C606.

[5] R. Fredriksson, M.C. Lagerstrom, L.G. Lundin and H.B. Schioth, The G-protein-coupled receptors in the human genome form five main families. Phylogenetic analysis, paralogon groups, and fingerprints, *Mol Pharmacol* **63** (2003), 1256–1272.

[6] Y. Hakak, D. Shrestha, M.C. Goegel, D.P. Behan and D.T. Chalmers, Global analysis of G-protein-coupled receptor signaling in human tissues, *FEBS Lett* **550** (2003), 11–17.

[7] S. Han and J. Roman, Suppression of prostaglandin E2 receptor subtype EP2 by PPARgamma ligands inhibits human lung carcinoma cell growth, *Biochem Biophys Res Commun* **314** (2004), 1093–1099.

[8] S.Y. Hsu, S.G. Liang and A.J. Hsueh, Characterization of two LGR genes homologous to gonadotropin and thyrotropin receptors with extracellular leucine-rich repeats and a G protein-coupled, seven-transmembrane region, *Mol Endocrinol* **12** (1998), 1830–1845.

[9] J.S. Kerley-Hamilton, A.M. Pike, N. Li, J. Direnzo and M.J. Spinella, A p53-dominant transcriptional response to cisplatin in testicular germ cell tumor-derived human embryonal carcinoma, *Oncogene* **24** (2005), 6090–6100.

[10] E. Kettunen, W. el-Rifai, A.M. Bjorkqvist, H. Wolff, A. Karjalainen, S. Anttila, K. Mattson, K. Husgafvel-Pursiainen and S. Knuutila, A broad amplification pattern at 3q in squamous cell lung cancer – a fluorescence in situ hybridization study, *Cancer Genet Cytogenet* **117** (2000), 66–70.

[11] H. Kiaris, A.V. Schally, A. Nagy, K. Szepeshazi, F. Hebert and G. Halmos, A targeted cytotoxic somatostatin (SST) analogue, AN-238, inhibits the growth of H-69 small-cell lung carcinoma (SCLC) and H-157 non-SCLC in nude mice, *Eur J Cancer* **37** (2001), 620–628.

[12] J. Koike, A. Takagi, T. Miwa, M. Hirai, M. Terada and M. Katoh, Molecular cloning of Frizzled-10, a novel member of the Frizzled gene family, *Biochem Biophys Res Commun* **262** (1999), 39–43.

[13] D. Kwekkeboom, E.P. Krenning and M. de Jong, Peptide receptor imaging and therapy, *J Nucl Med* **41** (2000), 1704–1713.

[14] D.K. Lee, T. Nguyen, K.R. Lynch, R. Cheng, W.B. Vanti, O. Arkhitko, T. Lewis, J.F. Evans, S.R. George and B.F. O'Dowd, Discovery and mapping of ten novel G protein-coupled receptor genes, *Gene* **275** (2001), 83–91.

[15] E.D. Loh, S.R. Broussard, Q. Liu, N.G. Copeland, D.J. Gilbert, N.A. Jenkins and L.F. Kolakowski Jr., Chromosomal localization of GPR48, a novel glycoprotein hormone receptor like GPCR, in human and mouse with radiation hybrid and interspecific backcross mapping, *Cytogenet Cell Genet* **89** (2000), 2–5.

[16] J. Machac, B. Krynyckyi and C. Kim, Peptide and antibody imaging in lung cancer, *Semin Nucl Med* **32** (2002), 276–292.
[17] S. Mazerbourg, D.M. Bouley, S. Sudo, C.A. Klein, J.V. Zhang, K. Kawamura, L.V. Goodrich, H. Rayburn, M. Tessier-Lavigne and A.J. Hsueh, Leucine-rich repeat-containing, G protein-coupled receptor 4 null mice exhibit intrauterine growth retardation associated with embryonic and perinatal lethality, *Mol Endocrinol* **18** (2004), 2241–2254.
[18] L.D. Miller, P.M. Long, L. Wong, S. Mukherjee, L.M. McShane and E.T. Liu, Optimal gene expression analysis by microarrays, *Cancer Cell* **2** (2002), 353–361.
[19] D.J. Moore, J.K. Chambers, J.P. Wahlin, K.B. Tan, G.B. Moore, O. Jenkins, P.C. Emson and P.R. Murdock, Expression pattern of human P2Y receptor subtypes: a quantitative reverse transcription-polymerase chain reaction study, *Biochim Biophys Acta* **1521** (2001), 107–119.
[20] Y. Nonaka, T. Hiramoto and N. Fujita, Identification of endogenous surrogate ligands for human P2Y(12) receptors by in silico and *in vitro* methods, *Biochem Biophys Res Commun* **337** (2005), 281–288.
[21] A. Onn and R.S. Herbst, Molecular targeted therapy for lung cancer, *Lancet* **366** (2005), 1507–1508.
[22] M. Palmer and E. Prediger, Assessing RNA Quality. In: TechNotes 11(1). Woodward, TX, USA: Ambion. The RNA Company, 2003: http://www.ambion.com/techlib/tn/111/118.html.
[23] D.M. Parkin, F. Bray, J. Ferlay and P. Pisani, Global cancer statistics, 2002, *CA Cancer J Clin* **55** (2005), 74–108.
[24] J. Pei, B.R. Balsara, W. Li, S. Litwin, E. Gabrielson, M. Feder, J. Jen and J.R. Testa, Genomic imbalances in human lung adenocarcinomas and squamous cell carcinomas, *Genes Chromosomes Cancer* **31** (2001), 282–287.
[25] D.C. Polacek, A.G. Passerini, C. Shi, N.M. Francesco, E. Manduchi, G.R. Grant, S. Powell, H. Bischof, H. Winkler, C.J. Stoeckert Jr. and P.F. Davies, Fidelity and enhanced sensitivity of differential transcription profiles following linear amplification of nanogram amounts of endothelial mRNA, *Physiol Genomics* **13** (2003), 147–156.
[26] C.A. Powell, A. Spira, A. Derti, C. DeLisi, G. Liu, A. Borczuk, S. Busch, S. Sahasrabudhe, Y. Chen, D. Sugarbaker, R. Bueno, W.G. Richards and J.S. Brody, Gene expression in lung adenocarcinomas of smokers and nonsmokers, *Am J Respir Cell Mol Biol* **29** (2003), 157–162.
[27] J.C. Reubi, Peptide receptors as molecular targets for cancer diagnosis and therapy, *Endocr Rev* **24** (2003), 389–427.
[28] J.C. Reubi, A. Kappeler, B. Waser, J. Laissue, R.W. Hipkin and A. Schonbrunn, Immunohistochemical localization of somatostatin receptors sst2A in human tumors, *Am J Pathol* **153** (1998), 233–245.
[29] J.C. Reubi, U. Laderach, B. Waser, J.O. Gebbers, P. Robberecht and J.A. Laissue, Vasoactive intestinal peptide/pituitary adenylate cyclase-activating peptide receptor subtypes in human tumors and their tissues of origin, *Cancer Res* **60** (2000), 3105–3112.
[30] R. Schafer, F. Sedehizade, T. Welte and G. Reiser, ATP- and UTP-activated P2Y receptors differently regulate proliferation of human lung epithelial tumor cells, *Am J Physiol Lung Cell Mol Physiol* **285** (2003), L376–L385.
[31] N. Shimizu, Y. Soda, K. Kanbe, H.Y. Liu, R. Mukai, T. Kitamura and H. Hoshino, A putative G protein-coupled receptor, RDC1, is a novel coreceptor for human and simian immunodeficiency viruses, *J Virol* **74** (2000), 619–626.
[32] S.G. Spiro and G.A. Silvestri, One hundred years of lung cancer, *Am J Respir Crit Care Med* **172** (2005), 523–529.
[33] T. Traub, V. Petkov, S. Ofluoglu, T. Pangerl, M. Raderer, B.J. Fueger, W. Schima, A. Kurtaran, R. Dudczak and I. Virgolini, 111In-DOTA-lanreotide scintigraphy in patients with tumors of the lung, *J Nucl Med* **42** (2001), 1309–1315.
[34] K. Uematsu, B. He, L. You, Z. Xu, F. McCormick and D.M. Jablons, Activation of the Wnt pathway in non small cell lung cancer: evidence of dishevelled overexpression, *Oncogene* **22** (2003), 7218–7221.
[35] Z. Wang, W. Shu, M.M. Lu and E.E. Morrisey, Wnt7b activates canonical signaling in epithelial and vascular smooth muscle cells through interactions with Fzd1, Fzd10, and LRP5, *Mol Cell Biol* **25** (2005), 5022–5030.
[36] E.R. Weibel, The pathway for oxygen. Structure and function in the mammalian respiratory system. 1st ed. Cambridge, Massachusetts: Harvard University Press, 1984.
[37] A. Wise, K. Gearing and S. Rees, Target validation of G-protein coupled receptors, *Drug Discov Today* **7** (2002), 235–246.
[38] T. Wittenberger, H.C. Schaller and S. Hellebrand, An expressed sequence tag (EST) data mining strategy succeeding in the discovery of new G-protein coupled receptors, *J Mol Biol* **307** (2001), 799–813.